Cell Reports, Volume *39*

Supplemental information

Disrupting the HDAC6-ubiquitin interaction impairs infection by influenza and Zika virus and cellular stress pathways

Longlong Wang, Etori Aguiar Moreira, Georg Kempf, Yasuyuki Miyake, Blandina I. Oliveira Esteves, Amal Fahmi, Jonas V. Schaefer, Birgit Dreier, Yohei Yamauchi, Marco P. Alves, Andreas Plückthun, and Patrick Matthias

Figure S1

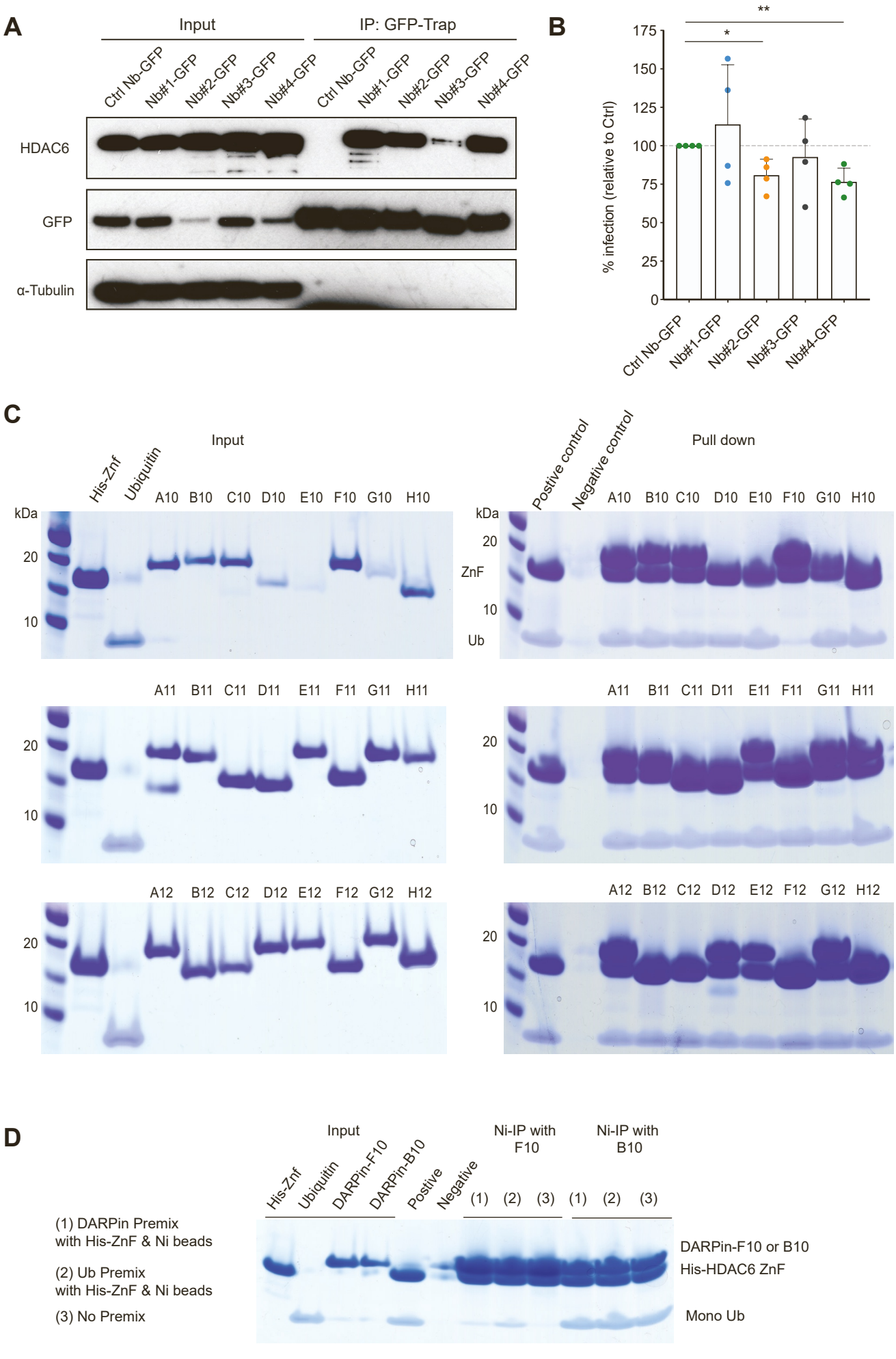
A
Input
IP: GFP-Trap
Ctrl Nb-GFP
Nb#1-GFP
Nb#2-GFP
Nb#3-GFP
Nb#4-GFP
HDAC6
GFP
α-Tubulin
B
% infection (relative to Ctrl)
C
Input
Pull down
His-Znf
Ubiquitin
Postive control
Negative control
kDa
ZnF
Ub
D
Input
Ni-IP with F10
Ni-IP with B10
DARPin-F10
DARPin-B10
Postive
Negative
(1) DARPin Premix with His-ZnF & Ni beads
(2) Ub Premix with His-ZnF & Ni beads
(3) No Premix
DARPin-F10 or B10
His-HDAC6 ZnF
Mono Ub

Figure S1 (related to Figure 1). HDAC6 ZnF interacting Nanobodies' effect on IAV infection and screen for DARPins blocking the HDAC6 ZnF-Ub interaction.

(A) A549 cells stably expressing nanobodies against HDAC6 ZnF were used for lysate preparation followed by pull-down with anti-GFP beads. The precipitate was analysed by SDS-PAGE and immunoblotted for HDAC6, GFP, and Tubulin. The input lanes were loaded with five percent of the lysate.

(B) IAV infection was analysed in A549 cells stably expressing the HDAC6 ZnF nanobodies (n=3). Infectivity was normalised to the control nanobody. Statistical analysis is done with One-way Anova, p-values refer to significant (<0.05) differences between samples. *, $p < 0.05$; **, $p < 0.01$. Data is represented as mean ± SD.

(C) Purified His-tagged HDAC6 ZnF (1108-1215), Flag-tagged DARPin candidates (A10-H10, A11-H11, A12-H12) and mono-ubiquitin were incubated together with Ni-NTA beads for 30 min, followed by precipitation and elution from the beads. Samples were analyzed by SDS-PAGE and visualized with Coomassie protein stain. As visible on the input panel, the size of the different DARPins varies slightly, depending on whether they have four or five loops. If a DARPin interacts with the ZnF domain without disturbing the binding of ubiquitin, pull-down of the ZnF domain via its His tag results in all three proteins being precipitated (pull-down panel). In the case of DARPin F10, ubiquitin is not precipitated, indicating that F10 binding interferes with ubiquitin binding.

(D) DARPin F10, and B10 as a control, were used for order of addition experiments. In (1) the DARPin was pre-mixed with His-ZnF, followed by ubiquitin addition 30 min later; in (2) Ub was pre-mixed with His-ZnF, followed by DARPin addition 30 min later; in (3) all three proteins were mixed together at the same time, followed by incubation for 60 min. Following the incubation, the ZnF domain was captured, and analysis was done by SDS-PAGE and Coomassie staining, as in (A) above. As shown, even when Ub is first pre-mixed with the ZnF domain, its binding is displaced by addition of DARPin F10.

Figure S2

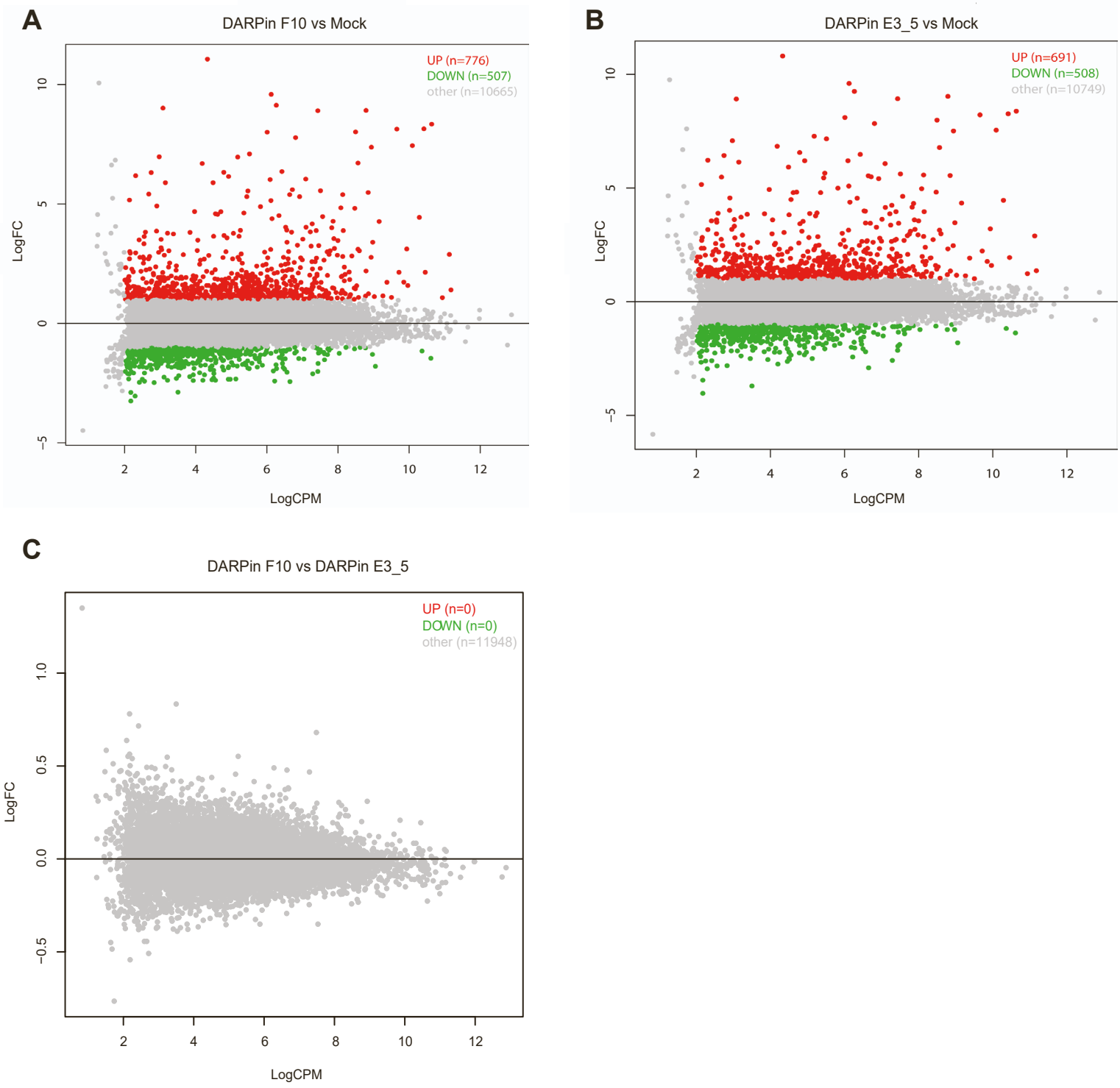

Figure S2 (related to Figure 1). Expression of DARPin F10 has no specific impact on gene expression

A549 cells were transiently transfected with GFP-tagged DARPin F10 or control DARPin E3_5, or mock transfected; three days after transfection GFP-positive cells were sorted by FACS and total RNA was extracted and analyzed by RNA-seq. The log2 fold change of the different pairwise comparisons (A, F10 vs mock-transfected; B, E3_5 vs mock-transfected; C, F10 vs E3_5) is displayed in MA plots. Differentially expressed genes (DEGs) are color-coded (fold change ≥1, FDR <0.01, logCPM >2): red (green) data points represent genes with higher (lower) expression level in DARPin-transfected cells vs mock-transfected cells. Comparison of the DEGs between F10 and E3_5 (C) shows that there are no specific gene expression changes between the two.

Figure S3

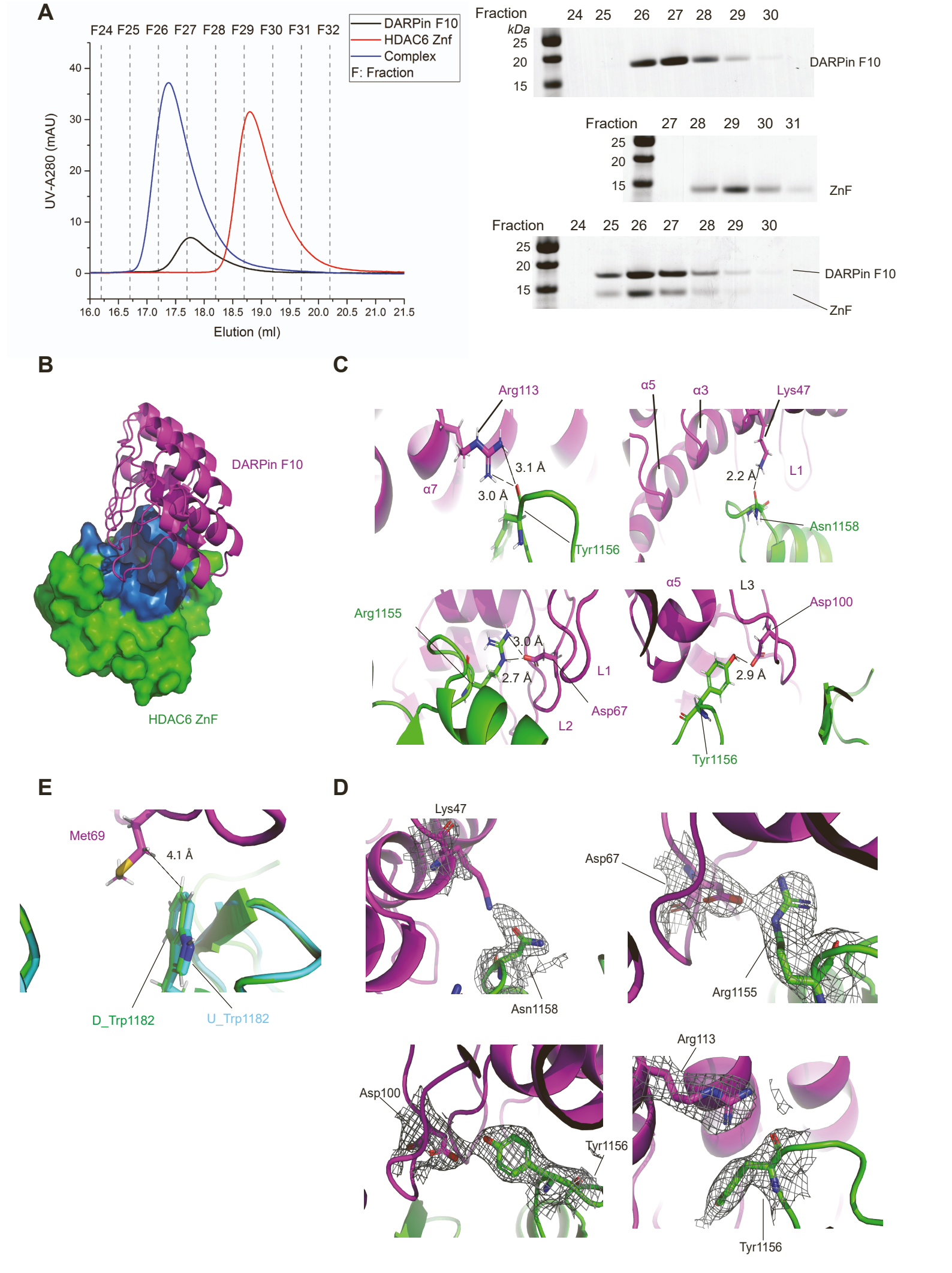
A
F24 F25 F26 F27 F28 F29 F30 F31 F32
DARPin F10
HDAC6 Znf
Complex
F: Fraction
UV-A280 (mAU)
Elution (ml)
Fraction
kDa
DARPin F10
ZnF
B
DARPin F10
HDAC6 ZnF
C
Arg113
α7
3.1 Å
3.0 Å
Tyr1156
α5
α3
Lys47
L1
2.2 Å
Asn1158
Arg1155
L2
Asp67
L3
Asp100
2.9 Å
D
Asp67
Arg1155
Asp100
E
Met69
4.1 Å
D_Trp1182
U_Trp1182

Figure S3 (related to Figure 2). DARPin F10 forms a stable complex with the HDAC6 ZnF domain.
(A) Size exclusion chromatography of purified DARPin F10 (black line), HDAC6 ZnF domain (red line) or the mixture of both (blue line). The upper graph shows the chromatographic profile. The lower panels show the analysis of indicated fractions by SDS-PAGE and Coomassie staining. The ZnF domain and DARPin F10 form a stable stoichiometric complex.
(B) DARPin F10 β-turns/loops insert into ZnF (shown with surface representation, ZnF coloured in green, canyon-like cleft of ZnF coloured in blue).
(C) Key amino acids involved in ZnF-DARPin F10 polar interactions. The hydrogen bonds are shown by dashed lines with distances indicated.
(D) The key residues involved in interaction between the ZnF domain and DARPin F10 are shown with a contour level = 1 and a carve (radius around each selected atom for which to include density) = 2.4 Å. Electron density is shown as grey grid. HDAC6 ZnF, green; DARPin F10, purple.
(E) Trp1182 is not affected by DARPin F10 binding. Met69 from DARPin F10 (magenta) is shown to measure the distance to Trp1182 of the ZnF domain. D_Trp1182: Trp1182 in DARPin-binding conformation (green); U_Trp1182: Trp1182 in Ubiquitin-binding conformation (cyan).

Figure S4

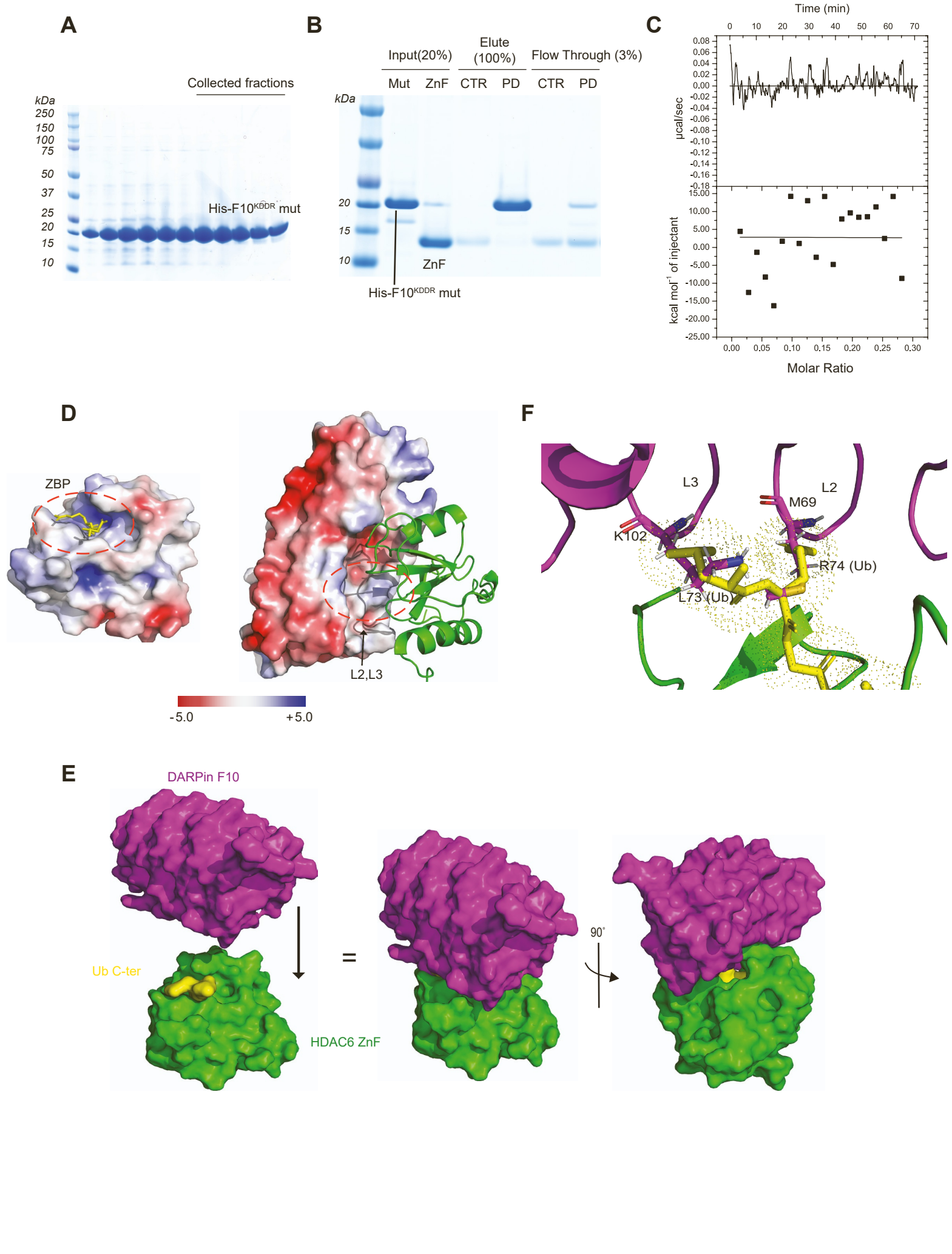
A
Collected fractions
kDa
250
150
100
75
50
37
25
20
15
10
His-F10KDDR mut
B
Input(20%)
Elute (100%)
Flow Through (3%)
Mut
ZnF
CTR
PD
CTR
PD
kDa
20
15
10
ZnF
His-F10KDDR mut
C
His-F10KDDR mut (0.1 mM) VS ZnF (0.01 mM)
Time (min)
µcal/sec
kcal mol-1 of injectant
Molar Ratio
D
ZBP
L2,L3
-5.0
+5.0
F
L3
L2
M69
K102
R74 (Ub)
L73 (Ub)
E
DARPin F10
Ub C-ter
HDAC6 ZnF
=
90˚

Figure S4 (related to Figure 2). DARPin F10^{KDDR} mutant does not bind to HDAC6 ZnF domain and Zoom-ins for DARPin F10 inhibition on Ub binding.

(A) Purification of mutant F10 by gel filtration. DARPin F10 was mutated at 4 residues (K47A, D67A, D100A, and R113A) to generate His-F10^{KDDR}. The protein was purified in gel filtration buffer (100 mM NaCl, 10 mM Tris pH=7.5, 2 mM TCEP) and the last 5 fractions were collected and pooled for further experiments.

(B) Pull down assay with HDAC6 ZnF(1108-1215). 10 µg His-F10^{KDDR} and 15 ug HDAC6 ZnF were incubated together; 10 µl Ni-NTA beads (slurry) were added to pull down the DARPin (and test whether the ZnF domain is carried along). Precipitated proteins were eluted with TBS buffer supplemented with 250 mM imidazole and analyzed by SDS-PAGE followed by staining with Instant Blue. Mut: His-F10^{KDDR}; ZnF, HDAC6 ZnF domain; CTR: Ni-NTA + HDAC6 ZnF; PD: Ni-NTA + HDAC6 ZnF + His-F10^{KDDR}.

(C) ITC to measure the affinity between His-F10^{KDDR} and HDAC6 ZnF. 0.1 mM and 0.01 mM protein were used respectively. No affinity was detected.

(D) Electrostatic surface potential map of the ZnF-Ub C-terminal complex structure (PDB: 3GV4). In the panel on the left, Ub is depicted as yellow sticks, showing that it fits into a positively charged pocket of the ZnF domain (ZnF electrostatic surface potential map is indicated). The ZnF Binding Pocket (ZBP) is shown. In the right panel, the electrostatic surface potential map of DARPin F10 is presented and the ZnF domain is shown (green). The region contacting the Ub-binding site (L2, L3, dashed circle) is neutral or slightly positively charged. Electrostatic surface potential maps were calculated with APBS (as PyMOL plugin) and range from -5 to +5 kT/e.

(E) Surface representation of the ZnF domain in complex with DARPin F10. Ubiquitin C-terminus is buried in the ZnF “canyon”. In the left panel, DARPin F10 and ZnF are moved apart for clarity. In the middle and right panels, the bound complex is shown, illustrating the occlusion of the Ub binding site by DARPin F10.

(F) DARPin F10 residues Lys102 (in L3) and Met69 (L2) occupy the space where the Ub C-terminus would engage. DARPin F10, purple; ZnF domain, green; Ub, yellow.

Figure S5

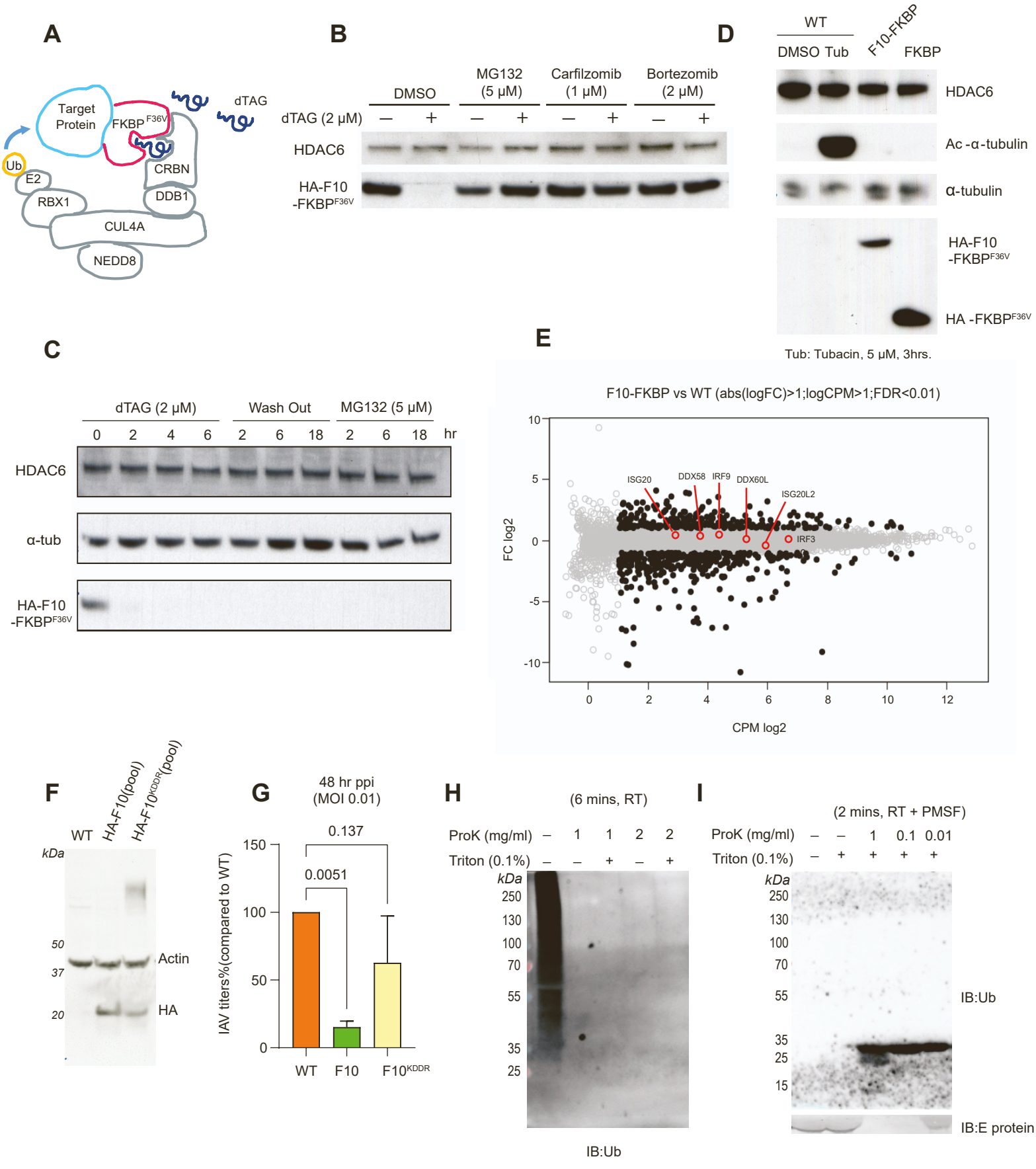
A
Target Protein
FKBP F36V
dTAG
Ub
E2
RBX1
CRBN
DDB1
CUL4A
NEDD8
B
DMSO
MG132 (5 μM)
Carfilzomib (1 μM)
Bortezomib (2 μM)
dTAG (2 μM) — + — + — + — +
HDAC6
HA-F10 -FKBP F36V
D
WT
F10-FKBP
DMSO Tub
FKBP
HDAC6
Ac -α-tubulin
α-tubulin
HA-F10 -FKBP F36V
HA -FKBP F36V
Tub: Tubacin, 5 μM, 3hrs.
C
dTAG (2 μM)
Wash Out
MG132 (5 μM)
0 2 4 6 2 6 18 2 6 18 hr
HDAC6
α-tub
HA-F10 -FKBP F36V
E
F10-FKBP vs WT (abs(logFC)>1;logCPM>1;FDR<0.01)
ISG20
DDX58
IRF9
DDX60L
ISG20L2
IRF3
FC log2
CPM log2
F
WT
HA-F10(pool)
HA-F10 KDDR (pool)
kDa
50
37
20
Actin
HA
G
48 hr ppi (MOI 0.01)
0.137
0.0051
IAV titers%(compared to WT)
WT
F10
F10 KDDR
H
(6 mins, RT)
ProK (mg/ml) — 1 1 2 2
Triton (0.1%) — — + — +
kDa
250
130
100
70
55
35
25
IB:Ub
I
(2 mins, RT + PMSF)
ProK (mg/ml) — — 1 0.1 0.01
Triton (0.1%) — + + + +
kDa
250
130
100
70
55
35
25
15
IB:Ub
IB:E protein

Figure S5 (related to Figure 3 & 4). Generation of inducible degraded DARPin F10 or F10^{KDDR} in A549 cells and ubiquitin presents in ZIKV particle.

(A) Scheme illustrating the the FKBP^{F36V}-dTAG system. The target protein is fused to a mutant version of the immunophilin FKBP, FKBP^{F36V}, which selectively binds to the small molecule dTAG-13. This allows recruitment of the Cereblon (CRBN) ubiquitin ligase complex, leading to ubiquitination and ensuing proteasomal degradation of the target protein.

(B) DARPin F10 degradation induced by dTAG is proteasome-dependent. When the F10 cell line was pre-incubated with proteasome inhibitors (MG132 5 µM, Carfilzomib 1 µM, Bortezomib 2 µM for 3 hrs, followed by dTAG treatment for 3 hrs), degradation of DARPin F10 was blocked.

(C) Once degraded, DARPin F10 does not stably reappear for at least 18 hours, even in the presence of proteasomal inhibition. A549 F10 cells were treated with dTAG to induce the degradation of DARPin F10; after 6 hours the medium was changed and replaced by normal medium (wash out) or medium containing MG132 (5 µM). Samples were analysed at different time points thereafter to monitor the re-expression of DARPin F10.

(D) F10 does not affect the enzymatic activity of HDAC6, as monitored by α-tubulin acetylation. The indicated cells (parental A549 cells, F10-FKBP cells and FKBP control cells) were used to examine the level of tubulin acetylation by immunoblotting. As a reference, A549 cells were treated with Tubacin (Tub; 5 µM, 3 hrs) to inhibit HDAC6 and elevate α-tubulin acetylation (2nd lane). The bottom panel shows the expression level of the DARPin F10-FKBP^{F36V} fusion protein, and of the FKBP^{F36V} control.

(E) RNA seq analysis between F10-FKBP cells and WT A549 cells. Genes that are upregulated or downregulated in DARPin F10 expressing cells are indicated in black. LogFC>1, LogCPM>1, FDR<0.05. Several interferon pathway genes are indicated, all of which show no significant change in expression.

(F) Generation of HA-F10 and HA-F10^{KDDR} cell lines. Lentivirus encoding HA-F10 and HA-F10^{KDDR} were used to transduce WT A549 cells and pools of puromycin-resistant cells were established. Cell lysates were used to visualize protein production by immunoblotting with an anti-HA antibody. Actin is an endogenous control.

(G) Wild-type F10, but not F10^{KDDR} mutant, reduces IAV infection. A549 WT, HA-F10 and HA-F10^{KDDR} cells were infected with IAV (MOI = 0.01) and viral titer in the culture medium was determined at 48 hr post infection by $TCID_{50}$ method (n=3). The baseline titer obtained with A549 WT cells was set to 100%. Statistical analysis was done with one-way ANOVA test, p-values are shown in the graph. Data are represented as mean ± SD.

(H) Optimization of proteinase K treatment on ZIKV particles. ZIKV (Puerto Rico strain; titer = 10^8/mL) was treated with proteinase K (RT°, 6 min) or Triton X-100 as indicated. Samples were analysed by immunoblotting with an anti-Ub antibody. The leftmost lane shows undigested material which exhibits a strong Ub smear signal. The proteinase K-treated samples were overdigested and no Ub signal is visible.

(I) Ubiquitin presence inside ZIKV particles. The same ZIKV strain (another preparation with lower titer = 10^7/mL) and reagents were used as in (A), but the proteinase K treatment was decreased to 2 min at RT° and immediately inactivated by 1 mM PMSF. The samples were analysed by immunoblotting with an anti-Ub antibody and anti-ZIKA E protein antibody.

Figure S6

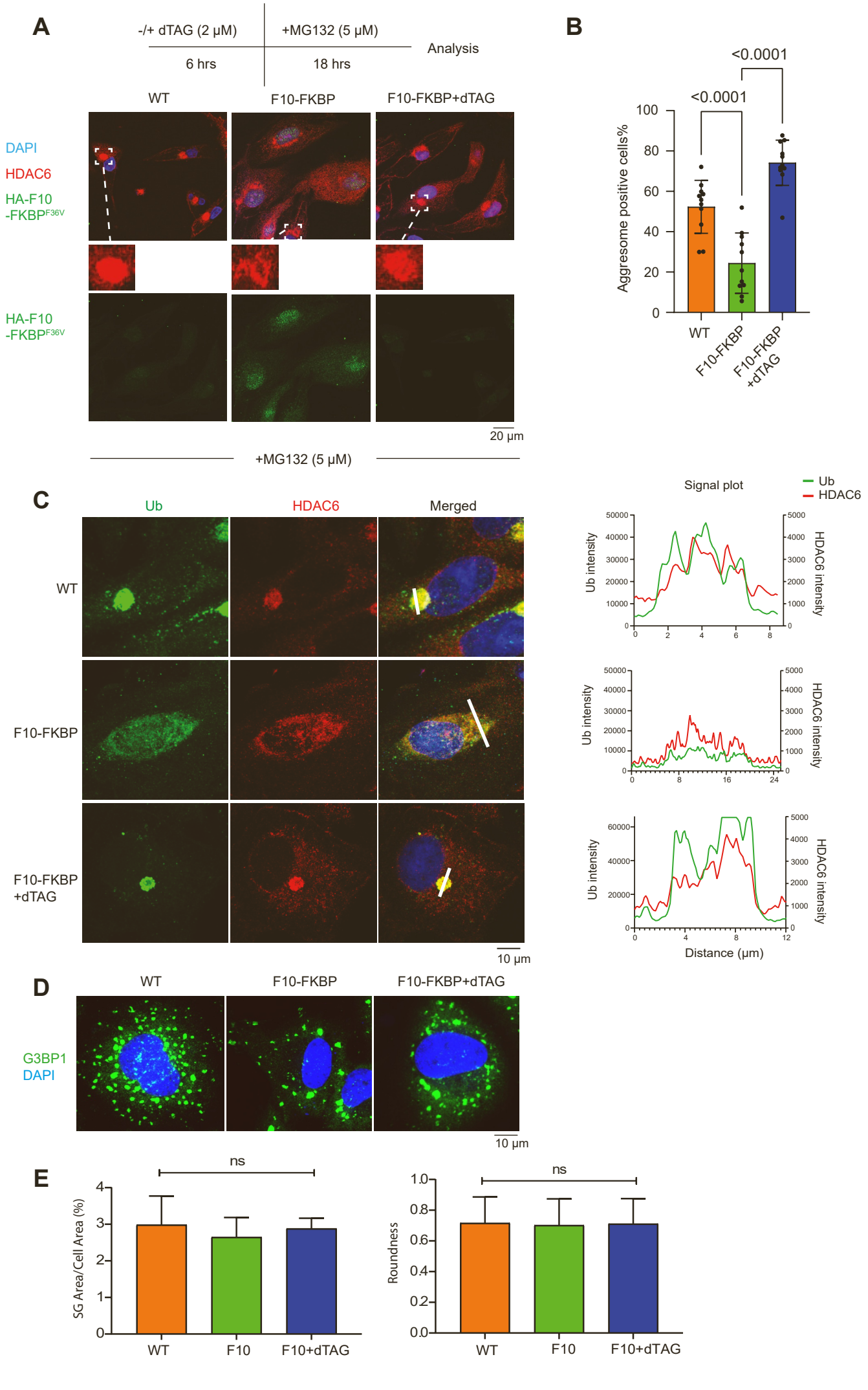
A
-/+ dTAG (2 μM)
+MG132 (5 μM)
Analysis
6 hrs
18 hrs
WT
F10-FKBP
F10-FKBP+dTAG
DAPI
HDAC6
HA-F10 -FKBP^F36V
HA-F10 -FKBP^F36V
20 μm
+MG132 (5 μM)
B
<0.0001
<0.0001
Aggresome positive cells%
100
80
60
40
20
0
WT
F10-FKBP
F10-FKBP +dTAG
C
Ub
HDAC6
Merged
WT
F10-FKBP
F10-FKBP +dTAG
10 μm
Signal plot
Ub
HDAC6
Ub intensity
HDAC6 intensity
Distance (μm)
D
WT
F10-FKBP
F10-FKBP+dTAG
G3BP1
DAPI
10 μm
E
ns
SG Area/Cell Area (%)
WT
F10
F10+dTAG
ns
Roundness
WT
F10
F10+dTAG

Figure S6 (related to Figure 5). Aggresome quantification with HDAC6 and representative pictures for aggresomes and SGs.

(A) Aggresome formation was induced with MG132 in parental A549 and F10-FKBP cells without or with dTAG pre-treatment to investigate the impact of the DARPin on aggresome formation. Aggresomes were detected by staining with an anti-HDAC6 antibody and DARPin F10 expression was visualized with an anti-HA antibody. DAPI was used to stain the nucleus. The inset shows a magnified view of an aggresome; representative pictures are shown. The scale bar represents 20 µm.

(B) Quantification of aggresome formation in parental A549 cells, or F10-FKBP cells without or with dTAG pre-treatment (n=2). The graph shows the percentage of aggresome-positive cells; each data point represents the percentage obtained in a randomly taken micrograph containing 50 to 100 cells. Statistical analysis was done by one-way ANOVA, p-values are shown in the graph. Data are represented as mean ± SD.

(C) Zoom-ins of aggresomes. Left and middle pictures illustrate the inhibition of aggresome formation by F10 (visualized by Ub and HDAC6 staining). The scale bar represents 10 µm.

The graphs on the right show the signal intensity for ubiquitin and HDAC6 across the aggresome or the perinuclear area (location shown as a white line in the pictures); note the different scale between Ub and HDAC6 signals.

(D) Example of F10 inhibition on SGs formation. Stress granules were visualized by staining with an anti-G3BP1 antibody (green). The scale bar represents 10 µm.

(E) SGs were induced with arsenite (1 mM, 30 min) in parental A549 cells or in F10-FKBP cells without or with dTAG pre-treatment (pre-incubation 2 µM for 6 hrs) and were visualized by staining for G3BP1. Representative pictures are shown in Figure 5. Left: quantification of the size of SGs per cell area. Right: shape (roundness) of SGs, as analyzed by ImageJ stress granule counter. Statistical analysis (n = 3) was done by one-way ANOVA test; ns, not significant. Data are represented as mean ± SD.

Table S2 Data collection and refinement statistics, Related to Figure 2

	DARPin F10-HDAC6 ZnF
Data collection [1]	
Space group	P 32 2 1
Cell dimensions	
a, *b*, *c* (Å)	81.39, 81.39, 103.64
α, β, γ (°)	90.00, 90.00, 120.00
Resolution (Å)	58.29 – 2.43 (2.63-2.43) [2]
R_{merge}	0.078 (1.883)
R_{pim}	0.033 (0.752)
$I / \sigma I$	19.0 (1.4)
$CC_{1/2}$ (%)	99.9 (58.9)
Wilson B-factor	64.61
Completeness (ellipsoidal)(%)	94.4 (75.6) [3]
Redundancy	10.5 (11.6)
Anomalous completeness (ellipsoidal)	94.4 (76.2)
Anomalous multiplicity	5.6 (6.2)
Experimental Phasing	
FOM [4] (%)	27.3
Refinement	
Resolution (Å)	58.29 – 2.43
No. reflections used in refinement	11396
R_{work} / R_{free} (%)	21.66/24.98
No. atoms (non hydrogen)	2054
Protein	2029
Ligand/ion	33
Water	10
B-factors (A^2)	78.11
Protein	78.26
Ligand/ion	69.18
Water	59.61
R.m.s. deviations	
Bond lengths (Å)	0.003
Bond angles (°)	0.59
Molprobity score	1.32
Clashscore	2.73
Ramachandran favored (%)	96.20
Ramachandran outliers (%)	0
Rotamer outliers (%)	0

1) Data collected from a single crystal
2) Values in parentheses are for the highest-resolution shell
3) From *STARANISO* assuming a local $I / \sigma I = 1.2$ resolution cutoff
4) Before density modification

Table S4. Oligonucleotide primers used in this paper, Related to STAR Methods

Primer name	Forward	Reverse
qPCR_RIG-I	AGCACTTGTGGACGCTTTA	GGTCATTCCTGTGTTCTGATTTG
qPCR_IFN-β	CTTCTCCACTACAGCTCTTTCC	GCCAGGAGGTTCTCAACAATA
qPCR_ISG15	GAGCATCCTGGTGAGGAATAAC	CGCTCACTTGCTGCTTCA
qPCR_IFN-γ	GGGTTCTCTTGGCTGTTACT	CTTGATGGTCTCCACACTCTT
qPCR_ZIKA E gene	CGYTGCCCAACACAAGG	CCACYAAYGTTCTTTTGCABACAT
qPCR_Actin	AGCCTCGCCTTTGCCGATC	AGCGGGCGATATCATCATCC
qPCR_GADPH	ACATCGCTCAGACACCATG	TGTAGTTGAGGTCAATGAAGGG
qPCR_18S	CGCCGCTAGAGGTGAAATTC	GGCAAATGCTTTCGCTCTG
pOPINF-His-HDAC6(1108-1215)	GGTCTGGAAGTTCTGTTTCAGGGCCCGACACCACTGCCCTGGTGTCCC	AATCACAAACTGGTCTAGAAAGCTTTAGTGTGGGTGGGGCATATCCTC
pOPINF-His-Avi-HDAC6(1108-1215)	AGCAGCGAATTCAGCGGCTTAAATGACATATTCGAAGCTCAGAAAATAGAGT	AATCACAAACTGGTCTAGAAAGCTTTAGTGTGGGTGGGGCATATCCTC
pLenti-Puro-Flag-HA-F10-FKBP^{F36V}	GCTGGTGGAGGTGGAGGTTCTGGATCCGACCTGGGTAAGAAACT	AGCTTGGTACCGAGCTCGGATCTTATTCCAGTTTTAGAAGCTCCACATC
pLenti-Puro-Flag-HA-FKBP^{F36V}	TTACGCTGGTGGAGGTGGAGGTTCTGGAGTGCAGGTGGAAACCATCTC	CTCCTCGCCCTTGCTCACCATTTCCAGTTTTAGAAGCTCCACATC
pcDNA3.1-GFP (1-9)	AATTCGCCACCATGGTGAGCAAGGG	AATTTTAGGGCAGCAGCACGGGGC
pcDNA3.1-GFP (10)-Ub	GGCCACCATGGACCTGCCAGACGA	CTCTAACCACCTCTCAGACGCAGGA
pcDNA3.1-GFP (11)-ZnF	TGGCCACCATGGAGAAGAGGG	TATGCCCCACCCACACTAAAG
pcDNA3.1-GFP (11)-ZnF （W1182A)	TGGCCACCATGGAGAAGAGGG	TATGCCCCACCCACACTAAAG
pcDNA3.1-mRuby	TATGGCTAGCATGACTGGT	ATTTAGGTGACACTATAG
Q5_F10_K47A	CCTGGCTGCTGACGCAGGTCACCT	TGCAGCGGAGTAACACCG
Q5_F10_D67A	AACGCTATCGCCATCATGGGTGC	AACGTCAGCACCGGTTTTCAGC
Q5_F10_D100A	CGCTATGGCCCATAAAGGTTTCA	TTAACGTCAGCGCCGGCCTT
Q5_F10_R113A	CTGGCTGCTTGGGCTGGTCACCT	GTGCAGCGGAGTGAAACCT
Plenti-HA-F10_WT & Mut	CCGACCTCTCTCCCCAGGGGGCCACCATGGTGTATCCGTATGATGTGCCGGAT	TAATCCAGAGGTTGATTGTCGATTAATTAAGCTTAGCAGCTTTCT